Force Measurements on Myelin Basic Protein Adsorbed to Mica and Lipid Bilayer Surfaces Done with the Atomic Force Microscope

Henning Mueller,* Hans-Jürgen Butt,# and Ernst Bamberg*
*Max-Planck-Institut für Biophysik, D-60596 Frankfurt(Main) and #Institut für physikalische Chemie, Universität Mainz, D-55099 Mainz, Germany

ABSTRACT The mechanical and adhesion properties of myelin basic protein (MBP) are important for its function, namely the compaction of the myelin sheath. To get more information about these properties we used atomic force microscopy to study tip-sample interaction of mica and mixed dioleoylphosphatidylserine (DOPS) (20%)/egg phosphatidylcholine (EPC) (80%) lipid bilayer surfaces in the absence and presence of bovine MBP. On mica or DOPS/EPC bilayers a short-range repulsive force (decay length 1.0–1.3 nm) was observed during the approach. The presence of MBP always led to an attractive force between tip and sample. When retracting the tip again, force curves on mica and on lipid layers were different. While attached to the mica surface, the MBP molecules exhibited elastic stretching behavior that agreed with the worm-like chain model, yielding a persistence length of 0.5 ± 0.25 nm and an average contour length of 53 ± 19 nm. MBP attached to a lipid bilayer did not show elastic stretching behavior. This shows that the protein adopts a different conformation when in contact with lipids. The lipid bilayer is strongly modified by MBP attachment, indicating formation of MBP-lipid complexes and possibly disruption of the original bilayer structure.

INTRODUCTION

The myelin sheath of the nervous system provides electrical insulation of the axon necessary for functional saltatory signal transduction (Huxley and Stampell, 1949). Myelin basic protein (MBP), located on the cytoplasmatic side of myelin membranes (Crang and Rumsby, 1978), is essential for the compaction of nervous system myelin to form the insulating myelin layer (Readhead et al., 1987). It is widely believed that MBP stabilizes opposing cytoplasmatic surfaces of membranes (Boggs et al., 1981; Fraser et al., 1989). The protein occurs in a number of different forms caused by different exon splicing (see Campagnoni, 1988 for a review) and various posttranslational modifications with possibly different roles in myelin formation (Staugaitis et al., 1996; Zand et al., 1998, and references therein). The most abundant variant in bovine central nervous system is termed 18.5 kDa/C1 for its molecular mass and position of its chromatography peak during purification. It is the subject of this investigation.

The interaction between MBP and the lipids in the membrane of cells forming the myelin sheath is important to understand the process of myelin compaction and has been studied using a variety of experimental techniques. Lipid vesicles and micelles have been reported to aggregate, fuse, or hemifuse in the presence of MBP (Lampe and Nelsestuen, 1982; Sedzik et al., 1984; ter Beest and Hoekstra, 1993; Jo and Boggs, 1995; Cajal et al., 1997). MBP exhibits random coil formation when dissolved in water (Smith, 1992; Krigbaum and Hsu, 1975; Mendz et al., 1984), but shows significant α-helical and β-sheet structure in the presence of lipids (Keniry and Smith, 1979, 1981; Mendz et al., 1990) with which it appears to interact hydrophobically (Boggs et al., 1986; Smith, 1992).

Beniac et al. (1997) have used MBP attachment to a lipid monolayer to determine MBP structure in this environment. They report a planar distribution of MBP on the monolayer with a toroidal shape of the MBP molecule of ~11 nm in diameter. MBP interaction with bilayers of different lipid compositions has been reported to be primarily ionic. Existence and magnitude of a hydrophobic electrostatic component in the interaction of MBP with bilayers are still under debate (Reinl and Bayerl, 1993; Cheifetz and Moscarello, 1985; Lampe and Nelsestuen, 1982; Nezil et al., 1992; Surewicz et al., 1987; Boggs et al., 1981; Nabet et al., 1994). It has been proposed that MBP links two apposing lipid bilayers together (Smith, 1977; Boggs et al., 1981). Whether the protein just sticks to the bilayer surface, penetrates into the head-group region, or penetrates deeper into the hydrophobic core of the bilayer has to be clarified yet (Smith, 1992; Reinl and Bayerl, 1993; Beniac et al., 1997).

During the last years the atomic force microscope (AFM) (Binnig et al., 1986) has turned out to be a valuable tool to study the properties of individual macromolecules (for a review see Manne and Gaub, 1997). Biological applications have included the determination of specific forces between ligands and receptors (Lee et al., 1994b; Moy et al., 1994; Florin et al., 1994), antigens and antibodies (Allen et al., 1996; Hinterdorfer et al., 1996; Browning-Kelley et al., 1997), complementary strands of DNA (Lee et al., 1994a) and between-cell adhesion proteins (Dammer et al., 1995), unfolding structural domains (Rief et al., 1997), the investigation of entropic exclusion in maintaining interfilament

Received for publication 17 August 1998 and in final form 9 November 1998.

Address reprint requests to Henning Mueller, Max-Planck-Institut für Biophysik, Kennedyallee 70, D-60596 Frankfurt(Main), Germany. Tel.: 49-69-6303-351; Fax: 49-69-6303-305; E-mail: mueller@wintermute.chemie.uni-mainz.de.

0006-3495/99/02/1072/08 $2.00

spacing (Brown and Hoh, 1997), or measuring changes in the interaction between a chaperonin and proteins (Vinckier et al., 1998).

Our goal was to determine the mechanical and adhesion properties of MBP. This might help to understand the physicochemical basis of the myelination process in which two apposed membranes adhere in the presence of MBP. Therefore, we measured the force between the tip of an AFM and a mica or lipid surface in the presence and absence of MBP.

MATERIALS AND METHODS

Reagents

All chemicals were of analytical grade and were used without further treatment. Chloroform, methanol, acetone, ethanol, hydrochloric acid, sulphuric acid, potassium chloride, potassium hydroxide, and sodium azide were obtained from Merck (Darmstadt, Germany). Glycine (ROTH, Karlsruhe, Germany), urea, phenylmethylsulfonyl fluoride (Sigma, Steinheim, Germany), sodium hydroxide, and sodium chloride (Fluka, Neu-Ulm, Germany) were also used. Buffer 1 (150 mM NaCl, 5 mM KH_2PO_4, pH 7.4, titrated with KOH) was used for AFM measurements except where specifically indicated. Buffer 2 (80 mM glycine, 6 M urea, pH 9.5, titrated with NaOH), buffer 3 (80 mM glycine, 2 M urea, pH 10.5, titrated with NaOH), and buffer 4 (80 mM glycine, pH 7.5, titrated with NaOH, 0.75 mM NaN_3) were used during protein purification.

Protein purification

MBP was purified following Beniac et al., 1997. Briefly, ~30 g of bovine brain white matter (obtained immediately after death and stored in liquid nitrogen until use) were homogenized in 280 ml of ice-cold chloroform/methanol (2:1, v/v). The homogenate was stirred overnight at 4°C and filtered through Whatman #1 filter paper under gravity in the fume hood at room temperature. The residue was washed twice with 130 ml of ice-cold chloroform/methanol, followed by 170 ml of ice-cold acetone. Then it was air dried and resuspended in 130 ml of 100 mM H_2SO_4, 0.1 mM phenylmethylsulfonyl fluoride and stirred gently overnight at 4°C. The suspension was centrifuged at 6000 × *g*, 4°C for 1 h, the supernatant collected, and the pellet resuspended in 50 ml of the same buffer and again centrifuged at 6000 × *g* at 4°C for 30 min. Supernatants were pooled and the protein precipitated by adding an equal volume of ice-cold ethanol. The mixture was left overnight at −20°C. The protein was recovered by centrifugation at 6000 × *g* for 30 min at −10°C. The pellet was resuspended in 10 ml of buffer 2 and dialyzed overnight against 500 ml of buffer 2 at room temperature. Insoluble material was removed by centrifugation at 6000 × *g* for 15 min at 4°C. The pH of the supernatant was adjusted to 9.5 with NaOH.

A preswollen and preequilibrated (buffer 2) Whatman CM-52 (sc Whatman, Maidstone, UK) anion exchange column (40 × 1 cm) was loaded with 10 ml of the extract at a rate of 6 ml/h at room temperature. After sample loading, the column was washed with 60 ml of buffer 2 at 12 ml/h for 5 h. The bound protein was eluted by 200 ml of buffer 3 in a linear gradient of 0–200 mM NaCl at 12 ml/h. The eluate was monitored at 280 nm and collected in 3-ml fractions. Under these conditions, the C1 component of MBP eluted last.

The C1 containing fractions were dialyzed two times against 1 l of buffer 4 at 4°C for 24 h. We estimated the protein content by the method of Lowry et al. (1951) and controlled the purity of the C1 component by sodium dodecyl sulfate-polyacrylamide gel electrophoresis (Fig. 1). The solution was stored in aliquots of 100 μl at −80°C until use.

Atomic force microscopy

Measurements were carried out with a commercial AFM (NanoScope™ 3, Digital Instruments, Santa Barbara, CA) and Si_3N_4 cantilevers (Digital Instruments, length 200 μm, width 40 μm, estimated thickness 0.6 μm, radius of tip curvature ~20–60 nm (Siedle et al., 1993)). Cantilever spring constants were individually determined by moving them against a reference cantilever according to Cleveland et al. (1993) and Preuss and Butt (1998), yielding values in the range of 0.06–0.14 N/m. Horizontal scanner calibration was performed by imaging the hexagonal crystal lattice of mica. In the vertical direction the scanner was calibrated as described by Jaschke and Butt (1995).

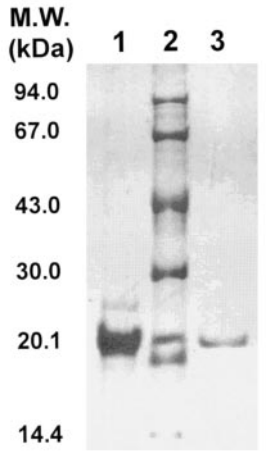

FIGURE 1 Sodium dodecyl sulfate-polyacrylamide gel electrophoresis of myelin basic protein. *Lane 1*: mixture of all charge isomers of MBP, this extract was loaded onto the CM-52 anion exchange column. *Lane 2*: Marker proteins. *Lane 3*: C1 containing fraction after chromatography. Basic proteins in this gel system run more slowly than predicted by their molecular mass (Beniac et al., 1997).

Sample preparation

Lipid vesicles for adsorption on mica were prepared as follows: dioleoylphosphatidylserine (DOPS) and egg phosphatidylcholine (EPC) dissolved in chloroform (Avanti Polar Lipids, Alabaster, AL) were mixed (1:4, v/v), and the solvent evaporated under N_2. Buffer 1 was added to the obtained lipid film to produce a 2-mg/ml suspension that was thoroughly sonicated (G112SP1T sonicator, Laboratory Supplies Co., Hicksville, NY) until the suspension became opalescent. Mica (Plano GmbH, Wetzlar, Germany) was freshly cleaved and mounted onto the AFM scanner. The silicone O-ring of the liquid cell was placed on top. An amount of 50 μl of vesicle suspension was pipetted onto the freshly cleaved mica inside the O-ring. After 10 min, the AFM head with liquid cell and tip was mounted and the cell volume (~200 μl including pipes) was rinsed with 1 ml of buffer 1 to remove vesicles not adsorbed to the mica. The system was left for 1–2 h to wait for the drift of the AFM signal offset to settle.

After taking data with the pure mica or lipid bilayer surface, 185 μl of MBP solution (0.8 mg/ml) were injected into the glass cell. After 10 min, the cell was rinsed again with 1 ml of buffer 1. The system was left for 30 min to wait for the drift of the AFM signal offset to settle. Force-versus-piezo displacement-plots were collected with NanoScope 3 Software v. 4.22r.

Force curves

In a force measurement, the sample is moved up and down by applying a voltage to the piezoelectric translator onto which the sample is mounted while measuring the cantilever deflection. The result of such a measurement is a force-versus-piezo displacement plot (Fig. 2 *a*), which shows the

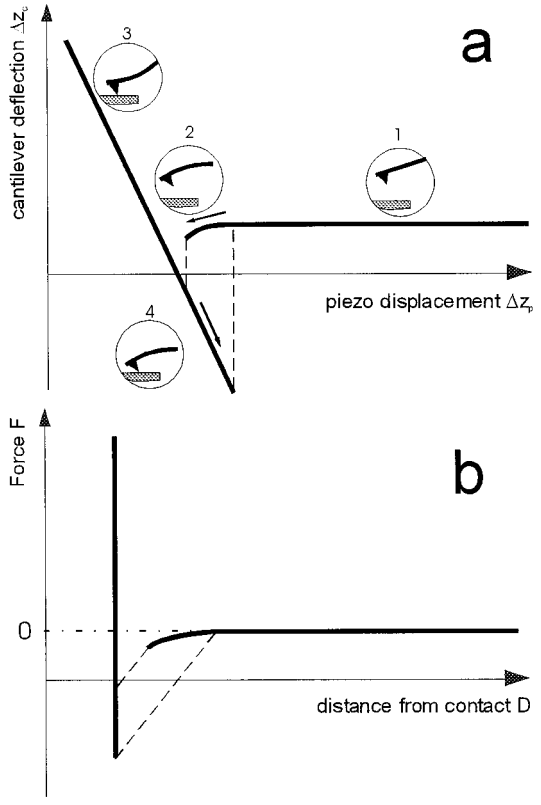

FIGURE 2 *a:* Sketch of a force-versus-piezo displacement plot for an attractive interaction and adhesion between tip and surface. A cycle in the force measurement starts at a large tip-surface separation (*1*). At large distances no force acts between tip and surface; the cantilever is not deflected while the surface moves. At smaller separations the assumed attraction pulls the cantilever toward the sample (*2*). At a certain point the tip often jumps onto the sample surface. This jump-in occurs when the gradient of attractive forces exceeds the spring constant plus the gradient of possibly present repulsive forces. Moving the sample further causes a deflection of the cantilever of the same amount as the sample is moved (constant compliance region, *3*). Finally, the surface is withdrawn to its starting position. During retraction the tip often sticks to the surface up to large distances because of adhesion (*4*) and then snaps out of contact. To obtain force-versus-distance curves (*b*) the original force-versus-piezo displacement-plots have to be converted by the relations $F = k\Delta z_c$ and $D = \Delta z_c + \Delta z_p$. k is the spring constant of the cantilever.

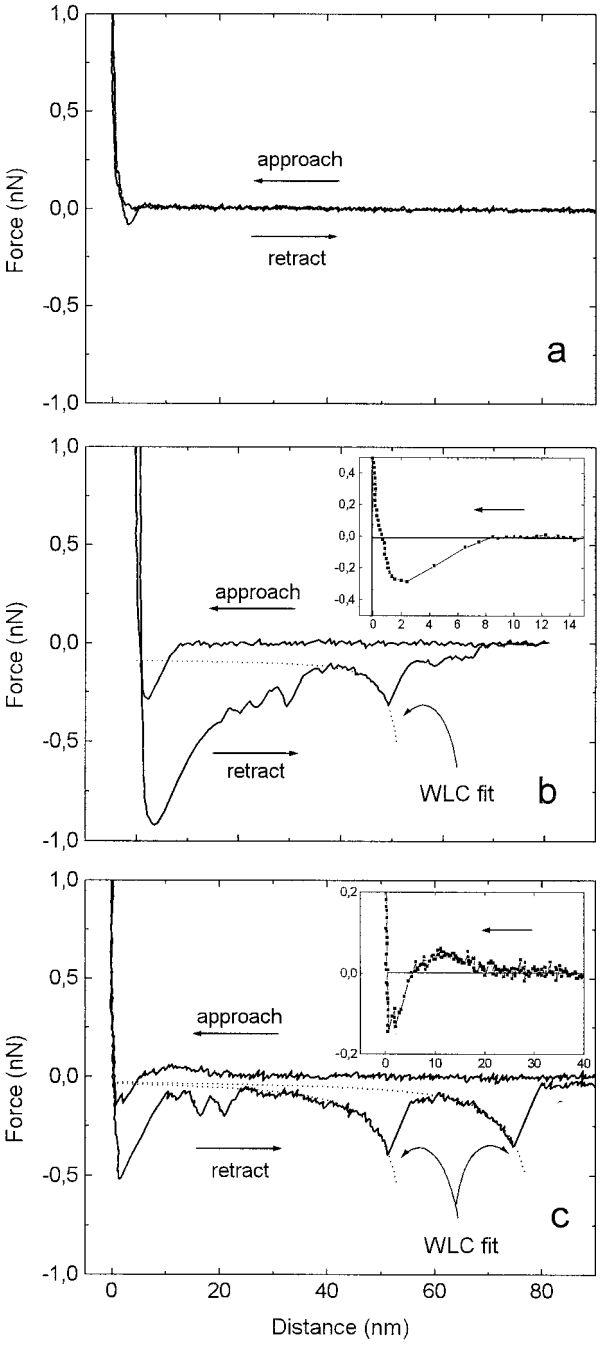

FIGURE 3 Force curves for bare mica (*a*) and MBP adsorbed from solution (*b* and *c*). The inset of *b* is a magnification of the approach up to 10 nm from contact. The extra lines show the zero force line and the contact line. The data for *a* and *b* was taken in buffer 1, whereas *c* was taken with a low ionic strength buffer (1 mM KCl). The inset in *c* shows that a repulsive interaction is present in the approach because of electrostatic double layer forces that are shielded by the high ionic strength of buffer 1 in *b*. A double exponential fit ($\lambda_{attractive} = 3.5$ nm, $\lambda_{doublelayer} = 8.5$ nm) for attraction and double layer repulsion is depicted in *c* (*inset*). WLC fits for the stretching processes in *b* and *c* are also given.

cantilever deflection Δz_c versus position of the piezo Δz_p. To obtain a force-versus-distance curve (Fig. 1 *b*, from now on called "force curve") from these data, Δz_c and Δz_p have to be converted into force and distance according to Fig. 2. Taking one force curve took ~1 s. This leads to approaching/retracting speeds of 1 μm/s.

Several numbers are derived from force curves, such as decay lengths or detachment forces. Then we report the error of a single measurement, not that of the mean value. This is to indicate typical fluctuations from force curve to force curve. We do not report the random error of the mean; because we did many experiments, it is negligible. It is also not relevant because the most significant uncertainty is probably of systematic nature.

RESULTS AND DISCUSSION

MBP adsorbed to a mica surface

A force curve taken on bare mica before adding MBP is shown in Fig. 3 *a*. In the approaching part of the force curve, no long-range forces acting over distances larger than 1 nm were observed. At close proximity, the tip was repelled (decay length <1 nm). Such a short-range repulsion was

observed earlier between two mica surfaces (Pashley and Israelachvili, 1981). It probably reflects the penetration of the tip into the thin layer of structured water and ions on the mica surface.

Upon retraction, a small adhesion was detected. It was probably caused by van der Waals forces. The electrostatic double layer force was negligible because of the high ionic strength. The small hysteresis of ~0.5 nm between the loading and unloading part in the contact regime is probably caused by a friction effect (Hoh and Engel, 1993).

When adding MBP at a concentration between 0.01 and 0.8 mg/ml, the force between tip and sample changed (Fig. 3 *b*). Upon approach, an attractive interaction was observed starting ~8 nm from contact and leading to a jump-in at a distance of ~4 nm. After this jump-in, a repulsive force of ~1 nm decay length was observed (Fig. 3 *b*, *inset*).

Before discussing the two force components, we would like to point out that both the mica and the tip surface were coated with adsorbed MBP. Hence, we measured an MBP-MBP interaction rather than MBP-silicon nitride interaction. Two observations support this view. First, when taking force curves in buffer of low ionic strength (1 mM KCl), an additional repulsive interaction was observed upon approach. This is caused by electrostatic double-layer forces that disappeared in buffer 1 because of shielding effects at high ionic strength. The MBP-coated mica surface is positively charged because of the high positive charge of MBP. Silicon nitride is negatively charged because of oxidation (Harame et al., 1987; Grattarola et al., 1992) (Although a study of Tsukruk and Bliznyuk (1998) reports a pK between 7 and 8 for Si_3N_4, we have observed a clearly electrostatic repulsion at low ionic strength between the silicon nitride tip and a mica surface at pH between 6.0 and 10.5 (data not shown). This proves that uncoated silicon nitride is negatively charged in our system.) This would lead to an electrostatic attraction. In order to explain a repulsion, silicon nitride also needs to be coated by the positively charged MBP. Second, when using silicon nitride as a substrate instead of mica, the same force curves were observed. Hence, the silicon nitride surface of the tip is also coated by a layer of adsorbed MBP.

The two force components observed in the presence of MBP, long-range attraction, and short-range repulsion, are discussed separately. The long-range attraction is probably not a van der Waals force. The formula $F = -RH/6D^2$ can be used to estimate the strength of the van der Waals attraction between a sphere of radius R at a distance D from a flat surface (Israelachvili, 1991). Using a Hamaker constant $H = 2 \times 10^{-20}$ J and a radius $R = 60$ nm, calculated forces were much smaller than measured forces. At $D = 3$ nm the calculated van der Waals force is only 0.02 nN. Therefore, the observed attraction is too strong to be attributed to van der Waals forces alone.

We believe that hydrophobic interactions are responsible for the long-range attraction. Although MBP does not contain extensive hydrophobic domains, it contains a high number of hydrophobic residues. That hydrophobic interactions are playing a role in MBP-MBP attraction has already been proposed by Afshar-Rad et al. (1987) based on surface force apparatus experiments. Afshar-Rad et al. found the attraction range to be larger than 17 nm. This can be attributed to different effective spring constants. Because of these, in the surface force apparatus the interacting surfaces jump into contact at a larger distance than in the AFM. In addition, heterogeneities like protruding proteins on the surface might play a role. Because of the large interaction areas in the surface force apparatus compared with the AFM, such heterogeneities could have a more drastic effect.

An alternative explanation for the attractive component could be a bridging effect or an attractive osmotic interaction between polypeptide segments protruding from the surface (see Patel and Tirell, 1989 for a review). Such attractive forces have been observed between polymer coated surfaces. However, we do not think that these effects play a significant role because the same attraction is observed with MBP on lipid bilayers (see below). For MBP on lipid bilayers we conclude from the retracting force curves that MBP adopts a relatively compact structure. Hence, any bridging force should be significantly different.

Retracting the tip, significant adhesion was observed that gradually decreased in strength over the first 20 nm. Receding the tip further, the force increased again, and one or more adhesion peaks were observed. This behavior provides evidence for the adsorption of MBP to the mica surface and the Si_3N_4 tip. The adhesion peaks are interpreted as detachment processes of individual MBP molecules that were picked up by the tip during contact. During retraction, the molecules were stretched until the applied force exceeded the adhesion between molecule and substrate and the molecule detached, leading to a sudden decrease of the force exerted on the cantilever. The elastic properties of these stretching events can be described with the worm-like chain (WLC, also known as the Porod-Kratky chain (Flory, 1989)) model for entropic elasticity. According to the WLC model, the force needed to stretch a linear polymer in a solvent to a length x is given by (Bustamante et al., 1994):

$$F(x) = (kT/b)[0.25(1 - x/L)^{-2} - 0.25 + x/L]$$

in which b is the persistence length (length of a stiff segment of the chain) and L is the contour length (length of the completely stretched chain). Our experiments yielded values $b = (0.50 \pm 0.25)$ nm and $L = (53 \pm 19)$ nm. The errors given are the ones of a single measurement, i.e., the width of the distribution of measured values.

These results agree with what is expected when stretching a polypeptide chain. The average distance between two C_α atoms of a polypeptide chain is 0.38 nm. This is the minimal size of a stiff element in a polypeptide chain and corresponds to b in the WLC model. A completely stretched chain of 169 amino acids (Eylar et al., 1971) has a length (contour length) of 64.2 nm.

It must be distinguished between contour length of the polypeptide chain and that of a stretching process. The

contour length of the chain is a property of the molecule and therefore constant. In the experimental setup, a polypeptide chain is adsorbed to mica at a random position *A* and is picked up by the tip at a random position *B* and then stretched. The contour length of the stretching process then is the contour length of the chain *A–B*, which is also random and smaller than that of the full chain. This leads to a broad distribution of measured contour lengths.

For evaluation, only stretching processes in the second half of the retraction curve were selected to avoid superposition of stretching forces from simultaneously attached polypeptide chains. In those cases in which more than one detachment in a single force curve was evaluated, the absolute force at the start of the first stretching process had to be equal to that at the start of the subsequent ones (Fig. 3 *c*). This means that the contour lengths of the different stretching processes were far from each other. For multiple stretching processes, this was almost always the case.

The distribution of the maximum distances of the last rupture process are shown in Fig. 4 *a*, the average value being 46 ± 15 nm. This maximal distance is also a random quantity depending on which part of the polypeptide chain is picked up in a single measurement. This leads to the large fluctuations around the mean that we have observed. The average detachment force was found to be 0.14 ± 0.06 nN. Detachment forces for single molecules have been reported for specific bonds (Florin et al., 1994; Moy et al., 1994; Dammer et al., 1995) and were comparable with ours. Reported strength for unspecific interaction was usually higher (1–10 nN) (Radmacher et al., 1994; Vinckier et al., 1998), but those numbers were based on the full adhesion observed immediately upon retraction. This corresponds to the lowest point in the retraction curve (e.g., Fig. 3 *b*) and can involve a large number of molecules.

In our case, the strength of the unspecific interaction is probably the adhesion between tip and a single molecule, F_{det} in Fig. 3 *b* and *c*. The adhesion to mica is stronger than the adhesion to silicon nitride because detachment forces observed in experiments with silicon nitride as a substrate showed the same result. If binding of MBP to mica were weaker than to silicon nitride, we would have expected lower detachment forces in the mica experiments. That binding of MBP to mica is stronger than to silicon nitride is expected because of the high surface energy and strong negative surface charge of mica.

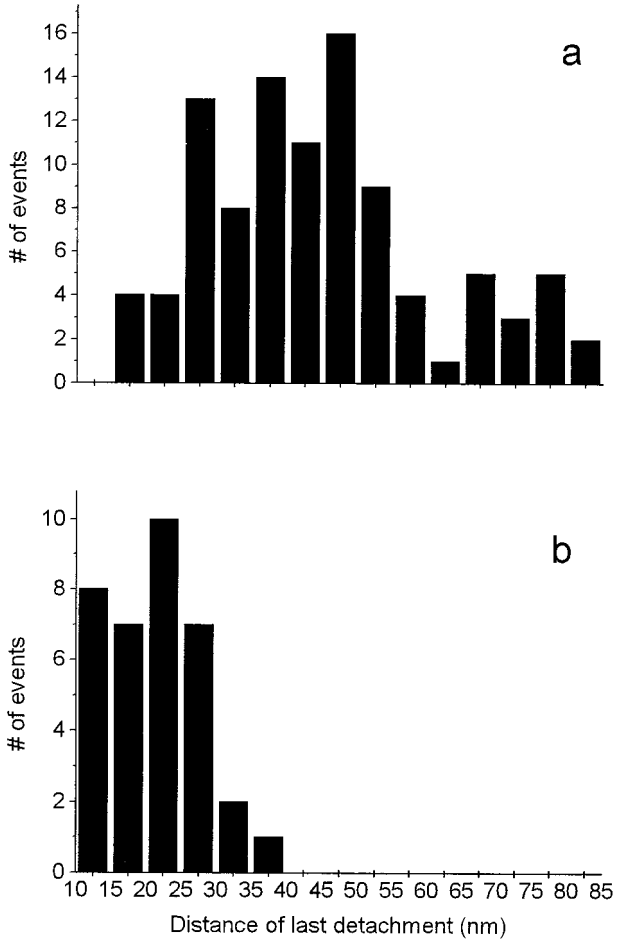

FIGURE 4 Distribution of the distances of the last detachment peak from contact for MBP on bare mica (*a*) and in the presence of a lipid bilayer (*b*). Values are significantly smaller in the presence of a lipid bilayer.

Lipid bilayer on mica

Vesicle adsorption forming bilayers on a solid substrate has been described by Brian and McConnell, 1984 and McConnell et al., 1986. On mica prepared with a vesicle suspension, the approaching tip experienced a repulsive force in buffer 1 (Fig. 5 *a*). This repulsion could be fitted with an exponential function and a decay length of 1.2 ± 0.2 nm. It can be electrostatics as well as the so-called hydration force (Marra and Israelachvili, 1985; McIntosh et al., 1987; Leikin et al., 1993; Israelachvili and Wennerström, 1996). The two effects lead to comparable decay lengths at this ionic strength.

On loads between 1 and 5 nN, the tip suddenly jumped onto the sample. The jump-in distance was either 4.2 ± 0.2 nm or 7.2 ± 0.4 nm.

From x-ray scattering experiments (McIntosh et al., 1987) the thickness of a fully hydrated EPC bilayer is known to be 6.3 nm and the headgroup-headgroup distance was determined to be 4.0 ± 0.04 nm. This is consistent with the 4.2 nm we have observed.

We believe that the jump-in is a penetration of the lipid bilayer by the tip (Ducker and Clarke (1994) on zwitterionic surfactants). This is supported by the observation that at high imaging forces, images of the underlying mica structure could be obtained, whereas at low forces this was not possible. Imaging the bilayer at minimum load showed a largely homogenous surface (up to 5 × 5 μm images were taken) with deposited material in some areas that could not be rinsed away (Ohlsson et al., 1995; our data not shown). The deposited material disappeared at high imaging forces.

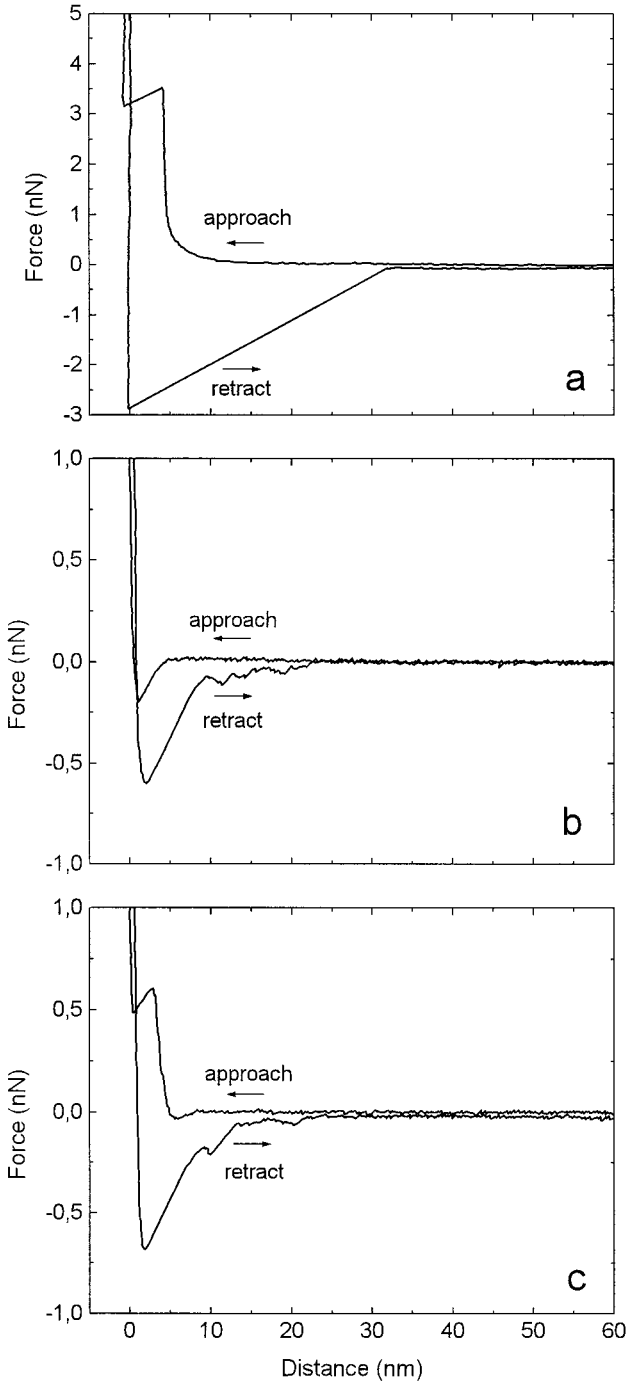

FIGURE 5 Force curves of (*a*) mica after bilayer deposition (*b*) type-1 curve and (*c*) type-2 curve after MBP adsorption to the bilayer. All curves were recorded in buffer 1.

Even in those areas in which no deposit was detected, force curves as in Fig. 5 *a* were always observed regardless of the position of the tip on the mica. Therefore, the surface seemed to be covered by a homogenous layer with occasionally additional lipid present on top.

The jump-in distance of 7.2 nm that we have observed was probably caused by the presence of lipid on the silicon nitride tip. Then, the tip penetrated both layers in one jump.

MBP binding to a EPC/DOPS lipid bilayer

Addition of MBP to the solution and subsequent flushing with buffer 1 resulted in significant changes to the force curves (Fig. 5 *b* and *c*). Two types of approach curves could be observed: type 1 was identical to the approach curve for MBP on mica without the presence of a lipid layer (Fig. 5 *b*). Type 2 showed a long-range attraction followed by a shorter-range repulsion and then a jump through a distance of ~3 nm (Fig. 5 *c*). Both types of curves appeared during one session of data collection at the same point of the surface (a possible piezo drift disregarded). Type 1 made up ~70%, and type 2 made up ~30% of all recorded curves. Both types were randomly distributed during data collection, an aging effect that caused one type to appear more often could not be inferred. In both cases, MBP present on lipid bilayer leads to an attractive force between tip and surface, which starts at ~5–8 nm.

We interpret the force curves in the following way. In type 2, the MBP is probably mainly on top of the bilayer. Hence, first the attraction caused by the lipid modified MBP is detected and at closer distance the tip penetrates the bilayer.

Type-1 force curves were probably obtained on bilayer that was destabilized by MBP. In other words, mica was covered with lipid-associated MBP. This is supported by the fact that the approaching force curves on a lipid bilayer equal those observed for MBP adsorbed on pure mica. In addition, a part-wise disruption of the DOPS/EPC layer has been reported for EPC bilayers by Roux et al. (1994), although in that study it did not occur when anionic lipids were present.

Alternatively, type-1 force curves could also be explained by the opposite effect, a stabilization of the bilayer by MBP. However, we do not think that this is the case because even at maximal forces of 23.5 nN, no jump-in was observed, and it is unlikely that a bilayer can withstand such high forces.

Summarizing, we believe that in the presence of MBP, two types of layers exist: a bilayer with MBP on top and MBP adsorbed to mica and associated with lipid. These two types are supposed to be in a dynamic equilibrium to account for the fact that even at one single position both types of force curves were observed.

Imaging the MBP-lipid bilayer surface with sufficient resolution was not successful up to now. Consequently, a dependence of force-distance-curve type on surface topology could not be inferred directly. Adsorption/desorption of material on the tip during the experiment might also be the cause for observation of the two different approach behaviors.

Retraction of the tip resulted in the same force-distance behavior regardless of the type of approach curve (Fig. 5 *b* and *c*). The detachment processes were, in any case, different from those on mica (Fig. 3 *b* and *c*). Elastic stretching was rarely observed. Detachment forces were 0.04 ± 0.02 nN, and the average distance of the last detachment peak from contact was found to be 21 ± 7 nm (Fig. 4 *b*). All of

these values were considerably smaller than those measured in the absence of lipids.

This shows that the structure of MBP without lipids is different from its structure in the presence of lipids. Without lipids, MBP behaves like a polymer chain in a good solvent. When lipids are present, it adopts a more compact structure. Appearance of secondary structure elements when lipids are present has been reported before (Keniry and Smith, 1979, 1981; Mendz et al., 1990; Mendz et al., 1995; and references therein). This should leave the protein more rigid than in random coil formation.

Such a refolding of MBP in the presence of lipids might also explain the lower detachment forces. Active sites on the polypeptide chain that are exposed when MBP is denatured are buried inside the protein after addition of lipids.

CONCLUSION

MBP present on mica and DOPS/EPC bilayers leads to an attractive interaction with the MBP-covered AFM tip, stronger than van der Waals interactions alone, and consistent with its ascribed role of compacting apposed membranes in myelin. Different stretching behavior indicates a structural change of the protein when in contact with lipids. Without lipids, MBP behaves like a polymer chain in a good solvent. Addition of lipids leads to a significantly more compact structure of MBP.

We are indebted to B. Löw (Oberhees) for making fresh bovine brain available, A. Eisenrauch, V. Heiselpetz, B. Legrum, and D. Ollig (Frankfurt) for help with column chromatography and gel electrophoresis, and M. Preuss (Mainz) for his expertise in determining cantilever spring constants. H. Mueller is supported by a grant from the Deutsche Forschungsgemeinschaft.

REFERENCES

Afshar-Rad, T., A. I. Bailey, P. F. Luckham, W. MacNaughtan, and D. Chapman. 1987. Forces between proteins and model polypeptides adsorbed on mica surfaces. *Biochim. Biophys. Acta.* 915:101–111.

Allen, S., X. Chen, J. Davies, M. C. Davies, A. C. Dawkes, J. C. Edwards, C. J. Roberts, J. Sefton, S. J. B. Tendler, and P. M. Williams. 1996. Detection of antigen-antibody binding events with the atomic force microscope. *Biochemistry.* 36:7457–7463.

Beniac, D. R., M. D. Luckevich, G. J. Czarnota, T. A. Tompkins, R. A. Ridsdale, F. P. Ottensmeyer, M. A. Moscarello, and G. Harauz. 1997. Three-dimensional structure of myelin basic protein I. *J. Biol. Chem.* 272:4261–4268.

Binnig, G., C. F. Quate, and Ch. Gerber. 1986. Atomic force microscope. *Phys. Rev. Lett.* 56:930.

Boggs, J. M., L. S. Chia, G. Rangaraj, and M. A. Moscarello. 1986. Interaction of myelin basic protein with different ionization states of phosphatidic acid and phosphatidylserine. *Chem. Phys. Lipids.* 39: 165–184.

Boggs, J. M., D. D. Wood, and M. A. Moscarello. 1981. Hydrophobic and Electrostatic interactions of myelin basic protein with lipid. participation of N-terminal and C-terminal portions. *Biochemistry.* 20:1065–1073.

Brian, A. A., and H. M. McConnell. 1984. Allogeneic stimulation of cytotoxic T cells by supported planar membranes. *Proc. Natl. Acad. Sci. USA.* 81:6159–6163.

Brown, H. G., and J. H. Hoh. 1997. Entropic exclusion by neurofilament side arms: a mechanism for maintaining interfilament spacing. *Biochemistry.* 36:15035–15040.

Browning-Kelley, M. E., K. Wadu-Mesthrige, V. Hari, and G. Y. Liu. 1997. Atomic force microscopic study of specific antigen/antibody binding. *Langmuir.* 13:343–350.

Bustamante, C., J. F. Marko, E. D. Siggia, and S. Smith. 1994. Entropic elasticity of λ-Phage DNA. *Science.* 265:1599–1600.

Cajal, Y., J. M. Boggs, and M. K. Jain. 1997. Salt-triggered intermembrane exchange of phospholipids and hemifusion by myelin basic protein. *Biochemistry.* 36:2566–2576.

Campagnoni, A. T. 1988. Molecular biology of myelin proteins from the central nervous system. *J. Neurochem.* 51:1–14.

Cheifetz, S., and M. A. Moscarello. 1985. Effect of bovine basic protein charge microheterogeneity on protein-induced aggregation of unilamellar vesicles containing a mixture of acidic and neutral phospholipids. *Biochemistry.* 24:1909–1914.

Cleveland, J. P., S. Manne, D. Bocek, and P. K. Hansma. 1993. A nondestructive method for determining the spring constant of cantilevers for scanning force microscopy *Rev. Sci. Instrum.* 64:403–405.

Crang, A. J., and M. G. Rumsby. 1978. Molecular organization in central nerve myelin. *Adv. Exper. Med. Biol.* 100:235–248.

Dammer, U., O. Popescu, P. Wagner, D. Anselmetti, H.-J. Güntherodt, and G. N. Misevic. 1995. Binding strength between cell adhesion proteoglycans measured by atomic force microscopy. *Science.* 267:1173–1175.

Ducker, W. A., and D. R. Clarke. 1994. Controlled modification of silicon nitride interactions in water via zwitterionic surfactant adsorption. *Colloids Surf.* 94:275–292.

Eylar, E. H., S. W. Brostoff, G. Hashim, J. Caccam, and P. Burnett. 1971. Basic A1 protein of the myelin membrane: the complete amino acid sequence. *J. Biol. Chem.* 246:5770–5784.

Florin, E. L., V. T. Moy, and H. E. Gaub. 1994. Adhesion forces between individual ligand-receptor pairs. *Science.* 264:415–417.

Flory, P. J. 1989. Statistical mechanics of chain molecules. Hanser, Munich. 401–403.

Fraser, P. E., R. P. Rand, and C. M. Deber. 1989. Bilayer-stabilizing properties of myelin basic protein in dioleoylphosphatidylethanolamine systems. *Biochim. Biophys. Acta.* 983:24–29.

Grattarola, M., G. Massobrio, and S. Martinoia. 1992. Modeling H^+-sensitive FETs with SPICE. *IEEE Trans. Electron Devices* 39:813–819.

Harame, D. L., D. L. Bousse, J. D. Shott, and J. D. Meindl. 1987. Ion-sensing devices with silicon nitride and borosilicate glass insulators. *IEEE Trans. Electron Devices* 34:1700–1707.

Hinterdorfer, P., W. Baumgartner, H. J. Gruber, K. Schilcher, and H. Schindler. 1996. Detection and localization of individual antibody-antigen recognition events by atomic force microscopy. *Proc. Natl. Acad. Sci. USA.* 93:3477–3481.

Hoh, J. H., and A. Engel. 1993. Friction effects on force measurements with an atomic force microscope. *Langmuir.* 9:3310–3312.

Huxley, A. F., and R. Stampell. 1949. Evidence for saltatory conduction in peripheral myelinated nerve fibers. *J. Physiol.* 108:315.

Israelachvili, J. N. 1991. Intermolecular and surface forces. Academic Press, London. 157–158.

Israelachvili, J. N., and H. Wennerström. 1996. Role of hydration and water structure in biological and colloidal interactions. *Nature.* 379: 219–225.

Jaschke, M., and H.-J. Butt. 1995. Height calibration of optical lever atomic force microscopes by simple laser interferometry. *Rev. Sci. Instrum.* 66:1258–1259

Jo, E., and J. M. Boggs. 1995. Aggregation of acidic lipid vesicles by myelin basic protein: dependence on potassium concentration. *Biochemistry.* 34:13705–13716.

Keniry, M. A., and R. Smith. 1979. Circular dichroic analysis of the secondary structure of myelin basic protein and derived peptides bound to detergents and lipid vesicles. *Biochim. Biophys. Acta.* 578:381–391.

Keniry, M. A., and R. Smith. 1981. Dependence on lipid structure of coil-to-helix transition of bovine myelin basic protein. *Biochim. Biophys. Acta.* 668:107–108.

Krigbaum, W. R., and T. S. Hsu. 1975. Molecular conformation of bovine A1 basic protein, a coiling macromolecule in aqueous solution. *Biochemistry.* 14:2542–2546.

Lampe, P. D., and G. L. Nelsestuen. 1982. Myelin basic protein-enhanced fusion of membranes. *Biochim. Biophys. Acta.* 693:320–325.

Lee, G. U., L. A. Chrisey, and R. J. Colton. 1994a. Direct measurement of the forces between complementary strands of DNA. *Science.* 266: 771–773.

Lee, G. U., D. A. Kidwell, and R. J. Colton. 1994b. Sensing discrete streptavidin-biotin interactions with atomic force microscopy. *Langmuir.* 10:354–357.

Leikin, S., V. A. Parsegian, and D. C. Rau. 1993. Hydration forces. *Annu. Rev. Phys. Chem.* 44:369–395.

Lowry, O. H., H. G. Rosebrough, A. L. Farr, and R. J. Randall. 1951. Protein measurement with the folin phenol reagent. *J. Biol. Chem.* 193:265–275.

Manne, S., and H. E. Gaub. 1997. Force microscopy: measurement of local interfacial forces and surface stresses. *Curr. Opin. Coll. Inter. Sci.* 2:145–152.

Marra, J., and J. Israelachvili. 1985. Direct measurements of forces between phosphatidylcholine and phosphatidylethanolamine bilayers in aqueous electrolyte solutions. *Biochemistry.* 24:4608–4618.

McConnell, H. M., T. H. Watts, R. M. Weis, and A. A. Brian. 1986. Supported planar membranes in studies of cell-cell recognition in the immune system. *Biochim. Biophys. Acta.* 864:95–106.

McIntosh, T. J., A. D. Magid, and S. A. Simon. 1987. Steric repulsion between phosphatidylcholine bilayers. *Biochemistry.* 26:7325–7332.

Mendz G. L., L. R. Brown, and R. E. Martenson. 1990. Interactions of myelin basic protein with mixed dodecylphosphocholine/palmitoyllysophosphatidic acid micelles. *Biochemistry.* 29:2304–2311.

Mendz, G. L., D. J. Miller, and G. B. Ralston. 1995. Interactions of myelin basic protein with palmitoyllysophosphatidylcholine: characterization of the complexes and conformations of the protein. *Eur. Biophys. J.* 24: 39–53.

Mendz, G. L., W. J. Moore, and R. E. Martenson. 1984. Interaction of myelin basic protein with micelles of dodecylphosphocholine. *Biochemistry.* 23:6041–6046.

Moy, V. T., E.-L. Florin, and H. E. Gaub. 1994. Intermolecular forces and energies between ligands and receptors. *Science.* 266:257–259.

Nabet, A., J. M. Boggs, and M. Pézolet. 1994. Study by infrared spectroscopy of the interaction of bovine myelin basic protein with phosphatidic acid. *Biochemistry.* 33:14972–14799.

Nezil, F. A., S. Bayerl, and M. Bloom. 1992. Temperature-reversible eruptions of vesicles in model membranes studied by NMR. *Biophys. J.* 61:1413–1426.

Ohlsson, P., T. Tjärnhage, E. Herbai, S. Löfås, and G. Puu. 1995. Liposome and proteoliposome fusion onto solid substrates, studied using atomic force microscopy, quartz crystal microblance and surface plasmon resonance: biological activities of incorporated components. *Bioelectrochem. Bioenerg.* 38:137–148.

Pashley, R. M., and J. N. Israelachvili. 1981. A comparison of surface forces and interfacial properties of mica in purified surfactant solutions. *Colloids Surf.* 2:169–187.

Patel, S. S., and M. Tirell. 1989. Measurement of forces between surfaces in polymer fluids. *Annu. Rev. Phys. Chem.* 40:597–635.

Preuss, M., and H.-J. Butt. 1998. Direct measurement of particle-bubble interactions in aqueous electrolyte: dependence on surfactant. *Langmuir.* 14:3164–3174.

Radmacher, M., M. Fritz, J. P. Cleveland, D. A. Walters, and P. K. Hansma. 1994. Imaging adhesion forces and elasticity of lysozyme adsorbed on mica with the atomic force microscope. *Langmuir.* 10: 3809–3814.

Readhead C., B. Popko, N. Takahashi, S. H. Shine, R. A. Saavedra, P. L. Sidman, and L. Hood. 1987. Expression of a myelin basic protein gene in transgenic mice: correction of the dysmyelination phenotype. *Cell.* 48:703–712.

Reinl, H. M., and T. M. Bayerl. 1993. Interaction of myelin basic protein with single bilayers on a solid support: an NMR, DSC and polarized infrared ATR study. *Biochim. Biophys. Acta.* 1151:127–136.

Rief, M., M. Gautel, F. Oesterhelt, J. M. Fernandez, and H. E. Gaub. 1997. Reversible unfolding of individual titin immunoglobulin domains by AFM. *Science.* 276:1109–1112.

Roux, M., F. A. Nezil, M. Monck, and M. Bloom. 1994. Fragmentation of phospholipid bilayers by myelin basic protein. *Biochemistry.* 33: 307–311.

Sedzik, J., A. E. Blaurock, and M. Höchli. 1984. Lipid/myelin basic protein multilayers: a model for the cytoplasmic space in central nervous system myelin. *J. Mol. Biol.* 174:385–409.

Siedle, P., H.-J. Butt, E. Bamberg, D. N. Wang, W. Kühlbrand, J. Zach, and M. Haider. 1993. Determining the form of atomic force microscope tips. *Inst. Phys. Conf. Ser. No.* 130:361–364.

Smith, R. 1977. Non-covalent cross-linking of lipid bilayers by myelin basic protein: a possible role in myelin formations. *Biochim. Biophys. Acta.* 491:581–590.

Smith, R. 1992. The basic protein of CNS myelin: its structure and ligand binding. *J. Neurochem.* 59:1589–1608.

Staugaitis, S. M., D. R. Colman, and L. Pedraza. 1996. Membrane adhesion and other functions for the myelin basic proteins. *Bioessays.* 18:13–18.

Surewicz, W. K., M. A. Moscarello, and H. H. Mantsch. 1987. Fourier transform infrared spectroscopy investigation of the interaction between myelin basic protein and dimyristoylphosphatidylglycerol bilayers. *Biochemistry.* 26:3881–3886.

ter Beest, M. B. A., and D. Hoekstra. 1993. Interaction of myelin basic protein with artificial membranes. *Eur. J. Biochem.* 211:689–696.

Tsukruk, V. V., and V. N. Bliznyuk. 1998. Adhesive and friction forces between chemically modified silicon and silicon nitride surfaces. *Langmuir.* 14:446–455.

Vinckier, A., P. Gervasoni, F. Zaugg, U. Ziegler, P. Lindner, P. Groscurth, A. Plückthun, and G. Semenza. 1998. Atomic force microscopy detects changes in the interaction forces between GroEL and substrate proteins. *Biophys. J.* 74:3256–3263.

Zand, R., M. X. Li, X. Jin, and D. Lubman. 1998. Determination of the sites of posttranslational modifications in the charge isomer of bovine myelin basic protein by capillary electrophoresis-mass spectroscopy. *Biochemistry.* 37:2441–2449.